Research Article

Journal of Environmental Nanotechnology

Response Surface Methodology-based Modeling and Optimization of AISI 1040 Turning Using Al_2O_3 and ZnO Nanofluids Under Minimum Quantity Lubrication

Altaf Nalbandh[1,2], Neeraj Chavda[3,4*] and Rakesh Bumataria[2]

[1]Department of Mechanical Engineering, Gujarat Technological University (GTU), Ahmedabad, GJ, India
[2]Department of Mechanical Engineering, Government Polytechnic, Porbandar, GJ, India
[3]Department of Mechanical Engineering, Gujarat Technological University (GTU), Ahmedabad, GJ, India
[4]Department of Mechanical Engineering, G. H. Patel College of Engineering and Technology, The Charutar Vidya Mandal (CVM) University, Vallabh Vidhyanagar, Anand, GJ, India
Received: 04.02.2026 Accepted: 16.02.2026 Published: 30.03.2026
*neeraj_chavda@yahoo.com

ABSTRACT

Nanofluid-based minimum quantity lubrication (MQL) supports near-dry machining by reducing fluid consumption while maintaining cooling and lubrication. This study examines Al_2O_3 and ZnO mono nanofluids under MQL in turning AISI 1040 steel, with cutting speed, feed rate, and nanoparticle weight percentage as inputs, and cutting force, cutting temperature, and surface roughness as responses. Experiments were designed using Box–Behnken response surface methodology, and quadratic models were validated through analysis of variance. Case A (Al_2O_3 + MQL) showed greater reductions in cutting force and surface roughness, whereas Case B (ZnO + MQL) provided better temperature control. Multi-response optimization for Case A identified low cutting speed (31.71 m/min), low feed (0.18 mm/rev), and 1 wt% nanoparticles as the best compromise among all three responses, supporting nanofluid-based MQL as a sustainable machining strategy.

Keywords: Nanofluids; Minimum quantity lubrication; Response surface methodology; Al_2O_3 and ZnO.

1. INTRODUCTION

Turning of medium carbon steels such as AISI 1040 requires precise dimensional control, smooth surfaces, and stable cutting forces. Conventional flood cooling, though effective in heat removal and lubrication, consumes large volumes of fluid, incurs disposal costs, and poses environmental and health risks. Its limited penetration into the tool workpiece interface further reduces efficiency. These drawbacks highlight the need for sustainable cooling and lubrication strategies that balance machining performance with ecological responsibility. Flood cooling in turning operations, though effective in heat removal, faces limitations due to excessive fluid use, disposal concerns, and poor accessibility at the cutting zone. Alternatives such as dry machining have been explored to eliminate fluid-related issues (Khan *et al.* 2018). More recently, Minimum Quantity Lubrication (MQL) has emerged as a practical and economical solution, reducing reliance on conventional coolants while improving tool–workpiece interaction (Abhang and Hameedullah, 2010). Mist lubrication, where a pressurized air–oil mixture is directed into the cutting zone, offers superior accessibility and lubrication efficiency (Sharma *et al.* 2015a). Further advancements include aerosol-based systems, which enhance cooling by spraying the lubricant coolant mixture directly at high pressure (Sharma *et al.* 2016b).

The comparative evaluation of MQL and wet machining of AISI 1045 steel was carried out using MINITAB's fractional factorial design to identify key factors, followed by response surface methodology (RSM) with a central composite design for optimization. The developed cutting force models showed good agreement with experimental results, whereas the surface roughness models did not (Hwang and Lee, 2010; Leppert, 2011). The authors evaluated dry, MQL, and emulsion cooling during the turning of AISI 1045 steel, reporting higher cutting forces under insufficient lubrication, particularly at low feed rates. (Haron *et al.* 2011) used RSM to study the influence of turning parameters on Inconel 718 surface integrity (roughness, microstructure, topography, microhardness), identifying feed rate as the dominant factor for roughness. (Hadad and Sadeghi, 2013) investigated MQL nozzle position and other parameters in turning AISI 4140 steel, finding it significantly lowered temperatures and forces. They validated a heat source/sink temperature model experimentally. (Liu *et al.* 2013) applied flexible coupling RSM under MQL, determining feed rate as the primary driver of surface roughness and cutting force, minimized at low feed/depth and high speed. (Saini *et al.*

2014) analyzed the effects of turning parameters on forces and tool-tip temperature in AISI 4340 steel using PVD and CVD inserts, with PVD-coated tools outperforming CVD. (Agrawal and Patil, 2018) compared aloe vera oil with conventional Servo Cut oil during machining of M2 steel, achieving a 6.7% reduction in surface roughness and a 0.14% decrease in tool wear with the bio-lubricant. (Sivaiah *et al.* 2020) compared MQL with textured *versus* untextured tools on AISI 52100 steel, reporting 42% roughness reduction, 40% flank wear decrease, and 25% lower cutting temperature using textured tools. (Singh *et al*. 2021) optimized turning of Hastelloy C-276 under vegetable oil MQL with RSM-CCD, identifying ideal parameters for minimal temperature, roughness, and maximal chip reduction coefficient. (Bhadoria and Bartarya, 2021) examined MQL with ceramic inserts on EN31 steel, which yielded superior surface roughness, reduced flank wear, and feasibility for high-speed/feed rates. (Sivaiah *et al*. 2021) demonstrated MQL with circular micro-pit textured tungsten carbide tools on AISI 304 steel, reducing roughness by 54%, tool wear by 7%, and boosting material removal rate by 27%.

Nanofluids, formed by dispersing solid nanoparticles in a base fluid, can significantly enhance the thermal and tribological performance of MQL systems by improving heat transfer and reducing friction at the tool–chip interface. Nanofluids, such as Al_2O_3, ZnO suspensions, utilize different nanoparticles to exploit synergistic effects, resulting in higher thermal conductivity, improved stability, and enhanced anti-wear and anti-friction properties (Bumataria *et al.* 2019 and 2020). These characteristics can translate into lower cutting temperatures, reduced cutting forces, and improved surface quality in metal cutting processes, yet the combined influence of process parameters and nanoparticle concentration on multi-response machinability in turning AISI 1040 under MQL remains insufficiently quantified. Response Surface Methodology, particularly Box–Behnken design, provides an efficient framework to model and optimize complex machining processes with a limited number of experiments by developing empirical relationships between inputs and multiple responses (Montgomery, 2013).

(Padmini *et al.* 2016) investigated the turning of AISI 1040 steel using nano boric acid (50 nm) lubricant suspensions in base oils such as SAE-40 and coconut oil. Nanofluid was prepared with different weight propositions at room temperature and mixed with a sonicator for one hour. The impacts of variations in machine cutting temperature, surface roughness, and average tool flank were studied. (Rao *et al.* 2011) investigated how cutting tool-workpiece cutting pressures, cutting temperatures, sample surface quality, and tool wear were affected by Carbon Nanotube (CNT) nanofluid when turning AISI 1040 steel. It was found in the results that the above parameters had a good effect, up to 2% CNT inclusion. (Amrita *et al.* 2013) investigated mist lubrication using nanographite (80 nm) during the turning of AISI 1040 steel with cemented carbide and HSS tools. For comparison, soluble oil was evaluated under dry, flood, and mist lubrication conditions without nanographite. The results showed significant retardation in tool wear and cutting forces with both cutting tools compared to dry and flood lubrication conditions. Furthermore, the findings of the experiment showed that using 0.5 wt% nano graphite with soluble oil and both cemented carbide and HSS cutting tools resulted in reduced cutting forces and tool wear at a flow rate of 15 mL/min.

The usage of graphite (80 nm), boric acid (100 nm), and MoS_2 (100 nm) nanoparticles in base fluid emulsifier oil was studied with minimum quantity lubrication in the turning of AISI 1040 steel by (Amrita *et al*. 2014). The stability of nanofluids containing 0.3 wt % nanoparticles was evaluated, and these cutting fluids were administered at 10 mL/min. (Sharma *et al.* 2016c; Sharma *et al.* 2016a) investigated how minimum quantity lubrication affected the machining of AISI 1040 steel using TiO_2 and Al_2O_3 nanoparticles distributed in a base fluid (vegetable oil + water emulsion). It resulted that with comparison to dry, mist, and wet machining, nanofluid machining resulted in considerable retardation in surface roughness and tool wear, as well as betterment in chip quality (silver-coloured chips with a curl and segmented morphology). (Rapeti *et al.* 2016) applied based fluids such as coconut oil, canola oil, and sesame oil with nano-cutting fluids containing MoS_2 nanoparticles to AISI 1040 steel turning. Grey Relational Analysis, which has its roots in the work of Taguchi, was applied to achieve multi-objective optimization. Coconut oil + 0.5% nano MoS_2 improved machining performance at 40 m/min machine cutting speed and a 0.14 mm/rev machine feed rate. (Pasam *et al.* 2018), experimentally studied developing and testing vegetable oil as a base fluid with micro and nano cutting fluids for turning of AISI 1040 steel in minimum quantity lubrication. Both boric acid (100 nm) and MoS_2 (90 nm) were dispersed in coconut oil base fluid. Nanofluids were superior to microfluidics at high cutting rates, but both performed similarly at lower speeds. Furthermore, MoS_2 was more effective than boric acid. (Padmini *et al.* 2019) focused on the performance testing of MoS_2-based nanofluids with various nanoparticle inclusions in vegetable oils (coconut, sesame, and canola) as a base fluid for machining AISI 1040 steel in an MQL environment. Cutting temperature, tool wear, cutting force, and surface roughness significantly decreased while 0.5% MoS_2 was blended into coconut, confirming better performance compared to additional lubricating strategies. (Sharma *et al*. 2015b) studied various concentrations of SiO_2 nanoparticles in vegetable oil and water emulsion base fluid to study their impact on the turning operation of AISI 1040 steel. Dry, MQL machining procedures were

tested in a variety of experiments. It has been demonstrated that dry machining and nanofluid + MQL reduce cutting force compared to operation in conventional cutting fluids. Furthermore, nanofluid + MQL retards surface roughness comparable to wet, traditional cutting fluid, and dry machining conditions.

Despite extensive research on nanofluid-assisted machining, most studies focus on either a single nanofluid, different work materials, or do not apply multi-response statistical optimization in a unified experimental framework. In particular, the comparative influence of Al_2O_3 and ZnO mono nanofluids under MQL on cutting force, cutting temperature, and surface roughness during turning of AISI 1040 steel has not been systematically quantified using RSM with Box-Behnken design. The present work addresses this gap by developing separate three factor, three response quadratic models for Al_2O_3 and ZnO nanofluids, and by identifying nanofluid specific optimal operating conditions in terms of cutting speed, feed, and nanoparticle weight percentage. This study therefore offers new insights into the selection and tuning of mono metal-oxide nanofluids for sustainable MQL-assisted turning of AISI 1040 steel.

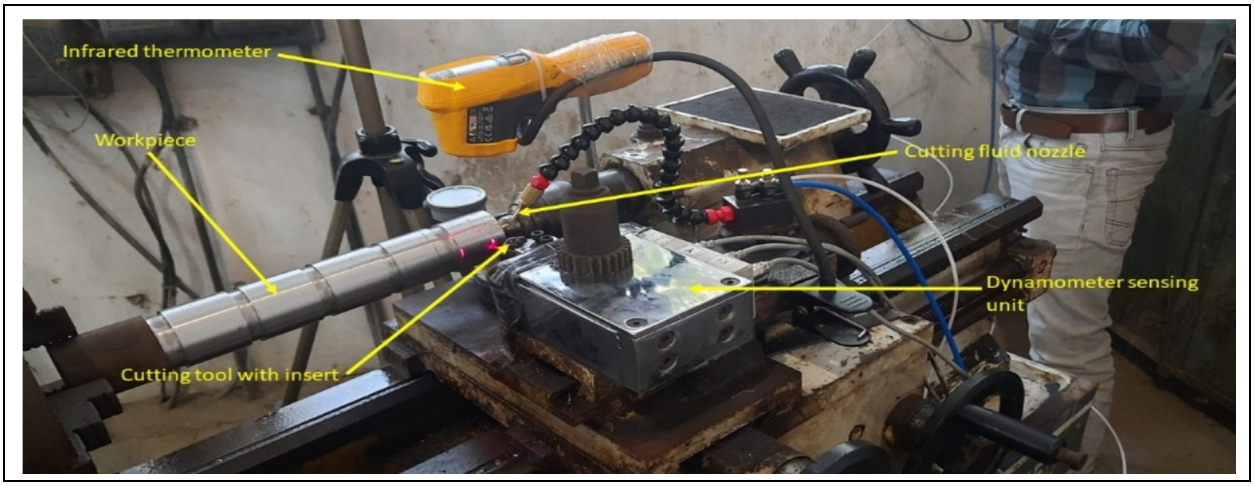


Fig. 1: Experimental setup

2. MATERIALS AND METHODS

In this study, design of experimentation (DOE) was done using RSM and study the effect of output parameters. The DOE facilitates the analysis of machining operations by minimizing time and costs through structured variation of factors. Three key inputs were examined: cutting speed (31.71, 69.63, 107.55 m/min), feed rate (0.11, 0.18, 0.25 mm/rev), and wt% nanofluid concentration (0%, 1%, 2%). All levels are detailed in Table 1.

Table 1. RSM Box Behnken method input parameters with their level

Input Parameters	Low (-1)	High (1)	Center (0)
Cutting speed (m/min)	31.71	107.55	69.63
Feed rate (mm/rev)	0.11	0.25	0.18
Wt% of nanoparticles (%)	0	2	1

For mono nanofluid preparation, Al_2O_3 and ZnO NPs of same size were mixed *via* the two-step method into 100 mL SAE-40 base fluid. Technical specification for both NPs is given in Table 2.

Table 2. Nanoparticle technical specification

Technical Specifications	Aluminium Oxide	Zinc Oxide
Molecular Formula	Al_2O_3	ZnO
Purity (%)	99.90	99.90
Average particle size (nm)	30-50	30-50
True Density (g/cm^3)	3.97	4.97
Bulk Density (g/cm^3)	1.5	-
Specific Surface area (m^2/g)	120-140	90-110
Molecular Weight (g/mol)	101.96	81.408
Morphology	Spherical	Spherical
Colour	White	Milky White
Physical form	Powder	Powder

The nanoparticle size range of 30–50 nm was chosen to provide sufficient thermal conductivity enhancement while minimizing agglomeration, thereby ensuring good dispersion and sprayability in MQL (Apmann *et al.* 2021). The nanoparticle concentration range of 0–2 wt% was chosen based on previous studies, which show that very low concentrations (<0.5 wt%) offer minimal enhancement, while higher concentrations (>1.5–2 wt%) increase viscosity, promote nozzle clogging, hinder atomization, and adversely affect surface finish and cutting forces (Günan *et al.* 2020).

Nanofluids were delivered *via* an MQL system featuring a reservoir, pressure valve, mixing chamber, and 2-mm nozzle, maintaining 3 bar air pressure and 360 mL/h flow rate. Experiments used AISI 1040 steel workpieces (Ø50 × 300 mm), with composition outlined in Table 3.

Table 3. Chemical composition (%) of workpiece

C	Si	Mn	P	S	Cr	Mo	Ni
0.43	0.26	0.8	0.03	0.02	0.23	0.08	0.05

Table 4. Details of experimentation and cutting conditions

Workpiece	
Material	AISI 1040 steel
Size	50 mm (Diameter) × 300 mm (Length)
Cutting fluid	
Cutting fluid	SAE-40 oil
Nanoparticles	
Aluminum oxide (Al_2O_3)	30-50 nm
Zinc oxide (ZnO)	30-50 nm
Weight percentage of nanoparticles	0%, 1%, 2%
Input Machining Parameters	
Cutting speed	31.71, 69.63, 107.55 m/min
Feed rate	0.11, 0.18, 0.25 mm/rev
Depth of cut	0.6 mm
MQL	
Nozzle diameter	2 mm
Nano fluid discharge	360 mL/h
Air Pressure	3 bar
Machine Tools and Measuring Devices	
Lathe	Banka 35 750 geared type
Cutting tool (insert)	Deskar TNMG160408 CQ LF9218
Cutting force	Dynamometer strain gauge based bridged form type
Cutting temperature	Fluke 62 Max+ digital infrared thermometer
Surface roughness	Mitutoyo SJ-210 portable tester

The Banka 35 750 geared lathe machine of Banka Machine Pvt. Ltd. was used for turning, and tool used was Deskar TNMG160408 CQ LF9218. A strain gauge-based bridge type lathe tool dynamometer was used to measure the cutting force. Also, for measuring cutting temperature, 62 Max+ digital infrared thermometer of Fluke was used. A portable surface roughness tester SJ-210 (Mitutoyo) was used to measure surface roughness of workpiece. In all the experiments, the depth of cut was kept fixed at 0.6 mm. Fig. 1 shows experimental setup used for performing test runs. Table 4 provides specifications of experiments.

Box-Behnken method was used for applying RSM in experimentation. Seventeen experiments were designed for each type of case of cooling method. Different cooling methods are given in Table 5.

Table 5. Cooling methods with type of NPs

Cooling Method	Type of NP with MQL
Case A	Al_2O_3
Case B	ZnO

Table 6. RSM tests and input and output values for case A

Run	Input Parameters			Output Parameters		
	A: CS	B: Wt% of Al_2O_3 NP	C: Fd	CF	CT	SR
	m/ min	%	mm/ rev	N	℃	µm
1	107.55	0	0.18	340.02	97.84	3.599
2	31.71	0	0.18	320.39	66.17	3.563
3	69.63	1	0.18	209.18	66.5	3.806
4	31.71	2	0.18	280.20	71.83	3.439
5	31.71	1	0.25	137.30	66.33	5.211
6	69.63	1	0.18	201.04	66	4.057
7	69.63	1	0.18	232.62	67.94	4.382
8	69.63	1	0.18	230.07	73.15	3.867
9	69.63	2	0.11	235.37	77.5	2.498
10	31.71	1	0.11	129.16	52.67	2.759
11	69.63	0	0.25	392.28	93.33	4.54
12	69.63	2	0.25	407.78	84.83	3.086
13	69.63	1	0.18	217.42	63.5	4.123
14	69.63	0	0.11	317.84	80.82	3.318
15	107.55	1	0.11	150.34	55	3.494
16	107.55	1	0.25	369.43	89.33	2.252
17	107.55	2	0.18	361.98	84.83	2.334

3. RESULTS AND DISCUSSION

Two different cooling methods (Case A & Case B), three input parameters such as cutting speeds (31.71, 69.93, and 107.55 m/min), feeds (0.11, 0.18, and 0.25 mm/rev), and weight percent (0, 1, and 2 wt%) were used. In total, 34 experiments were conducted on AISI 1040 steel. Cutting force, cutting temperature, and surface roughness were measured for each test run for each cooling method. The test runs, input and output values for Case A and Case B are given in Table 6 and **Error! Not a valid bookmark self-reference.**, respectively.

Table 7. RSM tests and input and output values for case B

Run	Input Parameters			Output Parameters		
	A: CS	B: Wt% of ZnO NP	C: Fd	CF	CT	SR
	m/ min	%	mm/rev	N	℃	µm
1	107.55	0	0.18	304.02	97.84	3.599
2	31.71	0	0.18	320.39	72	4.563
3	69.63	1	0.18	348.15	74	2.506
4	31.71	2	0.18	143.87	50.33	3.937
5	31.71	1	0.25	408.66	80	3.911
6	69.63	1	0.18	357.96	73	2.567
7	69.63	1	0.18	377.57	79.56	2.823
8	69.63	1	0.18	382.67	81.4	2.757
9	69.63	2	0.11	101.31	52.33	3.843
10	31.71	1	0.11	215.75	47	2.459
11	69.63	0	0.25	392.28	93.33	4.54
12	69.63	2	0.25	245.18	61.67	4.177
13	69.63	1	0.18	392.28	81	3.082
14	69.63	0	0.11	317.84	80.82	3.318
15	107.55	1	0.11	192.90	70	2.194
16	107.55	1	0.25	393.95	65	3.082
17	107.55	2	0.18	147.10	70	2.769

3.1 Analysis of Output Parameters for Case A

In this study of experimental research, cutting force and cutting temperature analysis was carried out during turning operation, whereas the analysis of surface roughness was carried out after end of operation. Additionally, statistical analysis was carried out using Design-Expert 13 software for output responses and normal probability and 3D surface plots were obtained.

3.1.1 Cutting Force

The software predicts a quadratic model and it is meaningful, as the p-value is less than 0.05. It means that whatever the p-value of a factor is lower, the factor is more meaningful than the rest of the factors. ANOVA for cutting force (Table 8) indicates that due to quadratic nature of model, square of wt% of NPs has p-value less than 0.0001 is more significant than wt% of NP with p-value 0.2455 and feed rate with p-value 0.0002.

Table 8. ANOVA for cutting force

Source	Sum of Squares	Mean Square	F-Value	p-Value	
Model	125100	13904.37	24.61	0.0002	significant
A-CS	15727.97	15727.97	27.84	0.0012	
C-Fd	28092.84	28092.84	49.72	0.0002	
AC	11124.82	11124.82	19.69	0.0030	
B^2	65442.30	65442.30	115.83	< 0.0001	
Residual	3954.89	564.98			
Lack of Fit	3229.78	1076.59	5.94	0.0590	not significant
Pure Error	725.11	181.28			
Cor Total	129100				

Fig. 2 shows the effect of all input parameters; A: cutting speed of 69.63 m/min, B: 1 wt% of NPs and C: feed of 0.18 mm/rev. As cutting speed and feed rate increase, cutting force also increases. The 3D response surface plot of wt% of NPs and cutting speed at feed rate 0.18 mm/rev is shown in Fig. 3. This shows minimum cutting force is at cutting speed 69.63 m/min and 1 wt% of NPs. It can also be seen that maximum amount of cutting force happens at 107.55 m/min and 0 wt% of NPs.

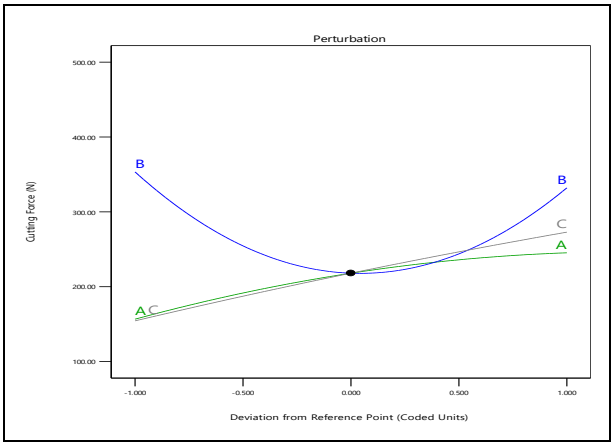


Fig. 2: Perturbation plot for cutting force

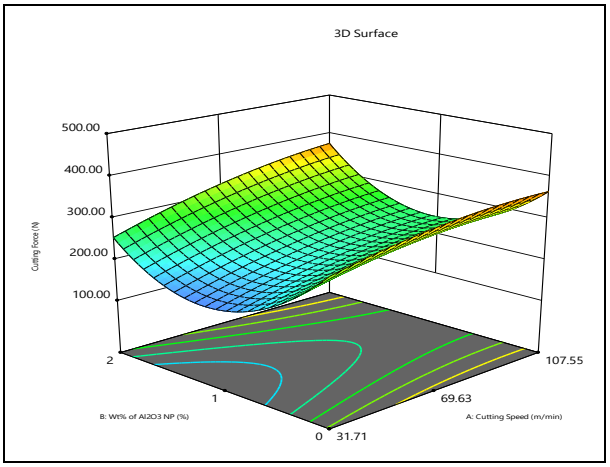


Fig. 3: 3D response surface plot cutting force *versus* cutting speed and wt% of Al_2O_3 NP

3.1.2 Cutting Temperature

For cutting temperature response, the software predicts a quadratic model and it is meaningful, as the p-value is less than 0.05. ANOVA for cutting temperature (Table 9) indicates that square of wt% of NPs, cutting speed and feed rate with p-value less between 0.0006 to 0.0028 are more significant and interaction between the factors are not significant. This model is a suitable model for output response cutting temperature drawn out from data in Table 9.

Table 9. ANOVA for cutting temperature

Source	Sum of Squares	Mean Square	F-Value	p-Value	
Model	2479.46	275.50	9.66	0.0034	significant
A-CS	612.50	612.50	21.48	0.0024	
C-Fd	575.11	575.11	20.17	0.0028	
B^2	1014.00	1014.00	35.55	0.0006	
Residual	199.64	28.52			
Lack of Fit	148.30	49.43	3.85	0.1128	not significant
Pure Error	51.33	12.83			
Cor Total	2679.09				

Fig. 4 shows the effect of all input parameters; A: cutting speed of 69.63 m/min, B: 1 wt% of NPs and C: feed rate of 0.18 mm/rev. It has same effect as cutting force, as cutting speed and feed rate increase, cutting temperature increases. Also, cutting temperature increases more at 0 and slightly at 2 wt% of NPs and cutting temperature decreases at 1 wt% of NPs.

The 3D response surface plot of wt% of NPs and cutting speed at feed rate 0.18 mm/rev is shown in Fig. 5. The minimum cutting temperature is at cutting speed 69.63 m/min and 1 wt% of NPs. It can also be seen that maximum amount of cutting temperature happens at 107.55 m/min and 0 wt% of NPs.

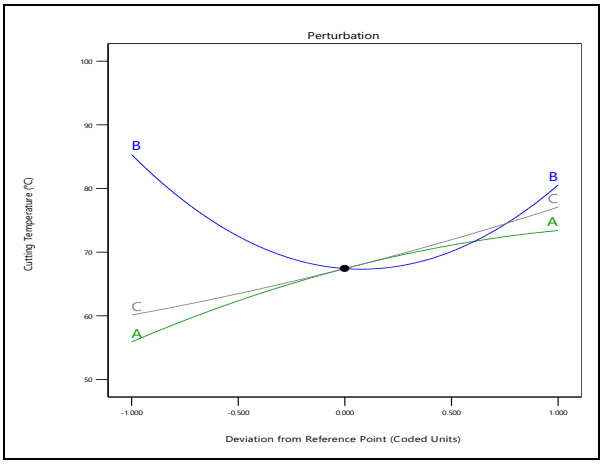


Fig. 4: Perturbation plot for cutting temperature

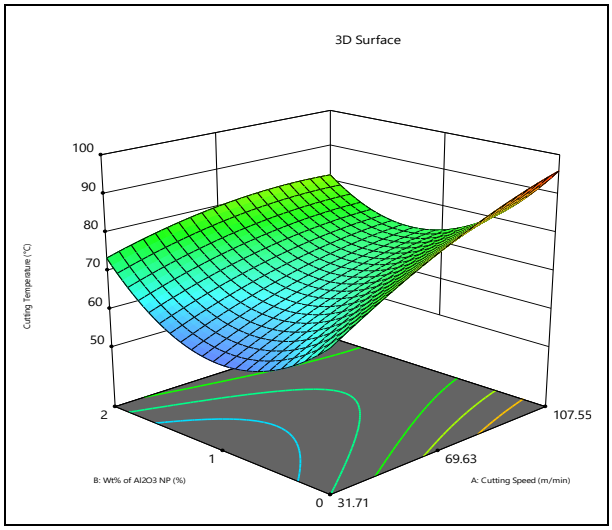


Fig. 5: 3D response surface plot cutting temperature *versus* cutting speed and wt% of Al_2O_3 NP

3.1.3 Surface Roughness

The software predicts a quadratic model for surface roughness of machined part. ANOVA for surface roughness (Table 10) indicates that interaction of cutting speed and feed rate are more significant followed by wt% of NPs and cutting speed.

Fig. 6 shows the effect of all input parameters; A: cutting speed of 69.63 m/min, B: 1 wt% of NPs and C: feed rate of 0.18 mm/rev. As cutting speed and wt% of NPs increase, surface roughness decreases. The 3D response surface plot of wt% of NP and cutting speed at feed rate 0.18 mm/rev is shown in Fig. 7. The minimum surface roughness is at cutting speed 107.55 m/min and 2 wt% of NPs. It can also be seen that maximum amount of surface roughness happens at 69.63 m/min and 1 wt% of NPs.

Table 10. ANOVA for surface roughness

Source	Sum of Squares	Mean Square	F-value	p-value	
Model	9.85	1.09	14.78	0.0009	significant
A-CS	1.36	1.36	18.31	0.0037	
B-Wt% of Al_2O_3 NPs	1.68	1.68	22.65	0.0021	
AC	3.41	3.41	46.08	0.0003	
Residual	0.5182	0.0740			
Lack of Fit	0.3097	0.1032	1.98	0.2593	not significant
Pure Error	0.2086	0.0521			
Cor Total	10.37				

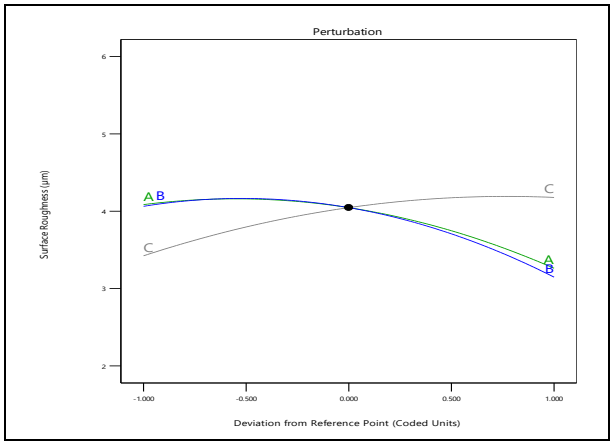


Fig. 6: Perturbation plot for surface roughness

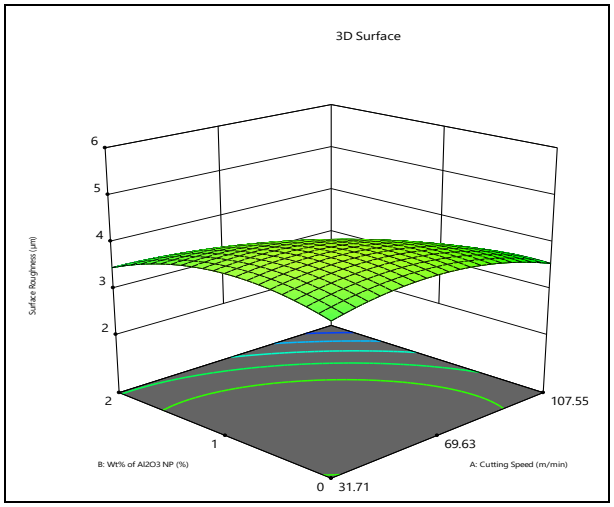


Fig. 7: 3D response surface plot surface roughness *versus* cutting speed and wt% of Al_2O_3 NP

Another important statistical measure used to evaluate the fitted models is the coefficient of determination (R^2) and its adjusted R^2. R^2 represents the proportion of variance in the response (dependent) variable explained by the set of predictors (independent variables). Although R^2 typically increases as more predictors are added to the model, this increase can occur even when the additional terms are not truly informative. Adjusted R^2 compensates for this by incorporating the number of predictors and degrees of freedom, thereby penalizing the inclusion of unnecessary variables. When both R^2 and adjusted R^2 are relatively high and close in value, the regression model is generally considered to have good explanatory power and to provide reliable predictions of the experimental response (Montgomery, 2013).

Table 11. Statistical indicators of proposed model for output responses of case A

Type	CF	CT	SR
R^2	0.9694	0.9255	0.9500
Adjusted R^2	0.9300	0.8297	0.8857
Predicted R^2	0.7909	0.6844	0.6906

As presented in Table 11, for all output responses, the R^2 and Adjusted R^2 values are both high and closely aligned, indicating that the proposed model provides a strong fit to the experimental data.

3.2 Analysis of Output Parameters for Case B

Similar to Case A, cutting force and cutting temperature analysis were carried out during turning operation, whereas the analysis of surface roughness was carried out after end of operation. Also, statistical analysis was carried out using Design-Expert 13 software for output responses and normal probability and 3D surface plots were obtained.

Table 12. ANOVA for cutting force

Source	Sum of Squares	Mean Square	F-Value	p-Value	
Model	160200	17798.10	23.21	0.0002	Signifi-cant
B-Wt% of ZnO NPs	60740.34	60740.34	79.22	< 0.0001	
C-Fd	46856.41	46856.41	61.12	0.0001	
B^2	34692.21	34692.21	45.25	0.0003	
Residual	5366.80	766.69			
Lack of Fit	4044.91	1348.30	4.08	0.1039	not signific-ant
Pure Error	1321.89	330.47			
Cor Total	165500				

3.2.1 Cutting Force

The software predicts a quadratic model and it is meaningful, as the p-value is less than 0.05. It means that whatever the p-value of a factor is lower, the factor is more meaningful than the rest of the factors. ANOVA for cutting force (Table 12) indicates that wt% of NPs with p-value less than 0.0001 are more significant than feed rate with p-value 0.0001 and square of wt% of NPs with p-value 0.0003.

Fig. 8 shows the effect of all input parameters; A: cutting speed of 69.63 m/min, B: 1 wt% of NPs and C: feed rate of 0.18 mm/rev. As feed rate increases, cutting force increases, while decreasing cutting speed and wt% of NPs decreases cutting force. The 3D response surface plot of wt% of NPs and cutting speed at feed rate 0.18 mm/rev is shown in Fig. 9. The minimum cutting force is at cutting speed 31.71 m/min and 2 wt% of NPs. It can also be seen that maximum amount of cutting force happens at 69.63 m/min and 1 wt% of NPs.

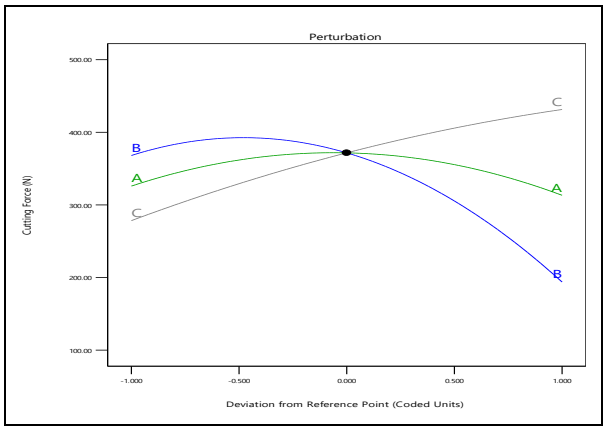


Fig. 8: Perturbation plot for cutting force

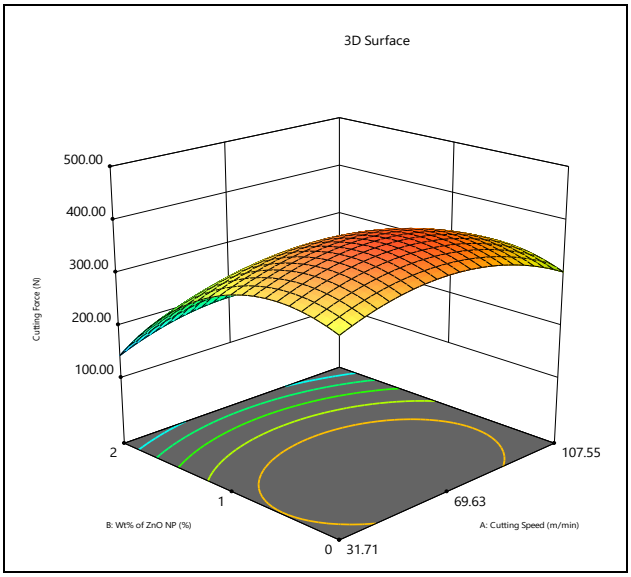


Fig. 9: 3D response surface plot cutting force *versus* cutting speed and wt% of ZnO NP

3.2.2 Cutting Temperature

For cutting temperature response, software predicts a quadratic model and it is meaningful, as the p-value is less than 0.05. ANOVA for cutting temperature (Table 13) indicates that wt% of NPs with p-value 0.0004 are more significant than other two input factors and interaction between the factors are not significant.

Table 13. ANOVA for cutting temperature

Source	Sum of Squares	Mean Square	F-value	p-value	
Model	2881.02	320.11	8.67	0.0047	significant
A-CS	357.92	357.92	9.69	0.0170	
B-Wt% of ZnO NP	1503.16	1503.16	40.70	0.0004	
C-Fd	310.63	310.63	8.41	0.0230	
Residual	258.53	36.93			
Lack of Fit	194.75	64.92	4.07	0.1042	not significant
Pure Error	63.78	15.94			
Cor Total	3139.55				

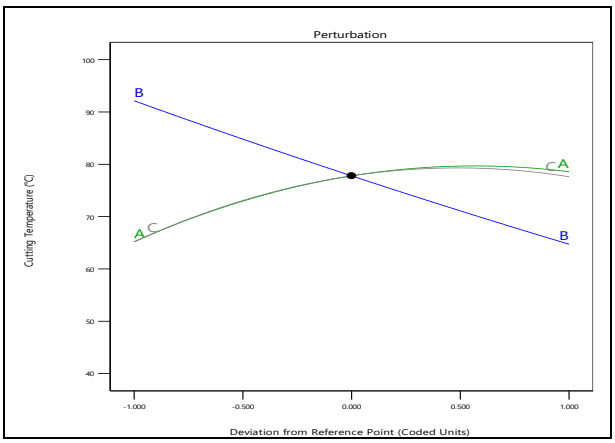


Fig. 10: Perturbation plot for cutting temperature

Fig. 10 shows the effect of all input parameters; A: cutting speed of 69.63 m/min, B: 1 wt% of NPs and C: feed rate of 0.18 mm/rev. As cutting speed and feed rate increase, cutting temperature increases. Also, cutting temperature decreases with increases in wt% of NPs. The 3D response surface plot of wt% of NPs and cutting speed at feed rate 0.18 mm/rev is shown in Fig. 11. The minimum cutting temperature is at cutting speed 31.71 m/min and 2 wt% of NPs. It can also be seen that maximum amount of cutting temperature happens at 107.55 m/min and 0 wt% of NPs.

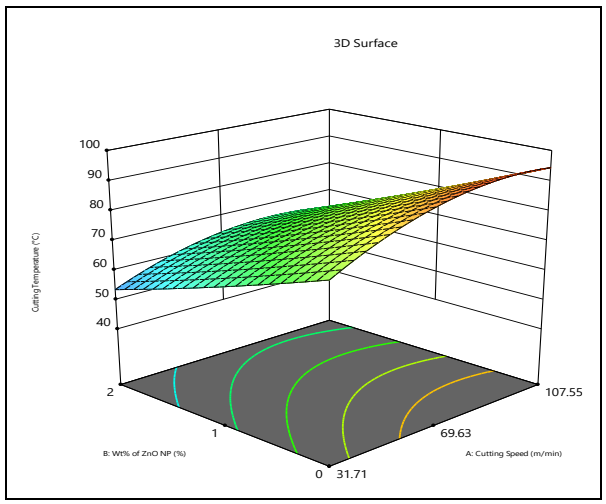


Fig. 11: 3D response surface plot cutting temperature *versus* cutting speed and wt% of ZnO NP

3.2.3 Surface Roughness

ANOVA for surface roughness (Table 14 highlights the squared terms of NPs wt% and feed rate as highly significant factors. Interactions between parameters exhibit no notable significance.

Table 14. ANOVA for surface roughness

Source	Sum of Squares	Mean Square	F-Value	p-Value	
Model	8.32	0.9240	8.65	0.0048	Significant
C-Fd	1.90	1.90	17.77	0.0040	
B^2	4.33	4.33	40.55	0.0004	
Residual	0.7473	0.1068			
Lack of Fit	0.5388	0.1796	3.44	0.1317	not significant
Pure Error	0.2086	0.0521			
Cor Total	9.06				

Fig. 12 shows the effect of all input parameters; A: cutting speed of 69.63 m/min, B: 1 wt% of NPs and C: depth of cut of 0.18 mm/rev. As feed rate and wt% of NPs increase, surface roughness increases. Furthermore, surface roughness showed an increased rate at 0 and 2 wt% of NPs and decreased rate at 1 wt% of NPs. Also, surface roughness decreases with increase of cutting speed.

The 3D response surface plot of wt% of NP and cutting speed at feed rate 0.18 mm/rev is shown in Fig. 13. The minimum surface roughness is at cutting speed 69.63 m/min and 1 wt% of NPs. It can also be seen that maximum amount of surface roughness happens at 31.71 m/min and 0 wt% of NPs.

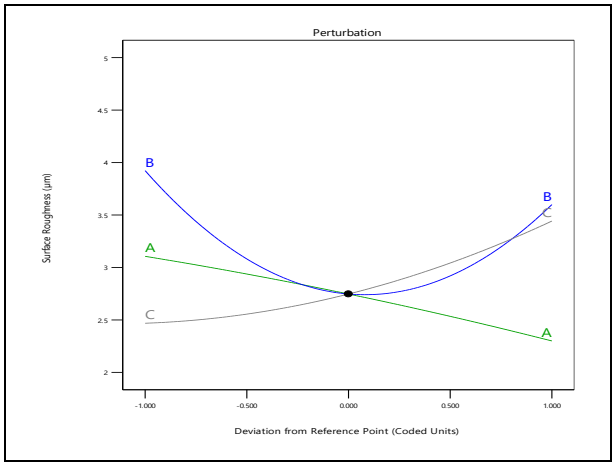


Fig. 12: Perturbation plot for cutting temperature

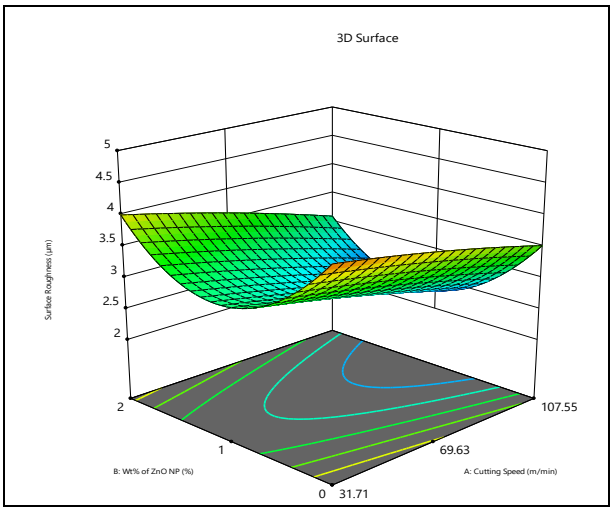


Fig. 13: 3D response surface plot surface roughness versus cutting speed and %wt of ZnO NP

As presented in Table 15, the R^2 and Adjusted R^2 values are both relatively high and closely aligned. This indicates that the proposed model provides a strong fit to the experimental data, thereby enhancing its reliability and predictive capability.

Table 15: Statistical indicators of proposed model for output responses of case B

Type	CF	CT	SR
R^2	0.9676	0.9177	0.9175
Adjusted R^2	0.9259	0.8118	0.8115
Predicted R^2	0.7966	0.6518	0.6815

The quadratic RSM–Box–Behnken models developed for cutting force, cutting temperature, and surface roughness demonstrated strong adequacy, with high coefficients of determination and non-significant lack-of-fit values. This confirms the reliability of the models in capturing the influence of machining

parameters and nanofluid composition on performance outcomes. A clear distinction emerged between the two nanofluid systems. In Case A, Al_2O_3 nanofluid consistently yielded lower surface roughness values, particularly at low to moderate feed rates and intermediate nanoparticle concentrations. This improvement can be attributed by forming a protective tribo-film and acting as micro bearings, thereby reducing friction and cutting force behaviour of Al_2O_3 nanoparticles, which enhance tribological performance (Sharma *et al.* 2016a). The reduction in cutting force and improved surface finish highlight the suitability of Al_2O_3 nanofluid when tool wear and surface integrity are prioritized. Conversely, Case B with ZnO nanofluid influenced cutting temperature more strongly due to its superior heat conduction capability, dissipating thermal energy efficiently at higher cutting speeds. The high thermal conductivity of ZnO nanoparticles enhance heat transfer from the tool workpiece interface into the fluid, dissipating thermal energy more effectively at elevated cutting speeds (Shaikh *et al.* 2024). In contrast, Al_2O_3 nanofluid (Case A) primarily improves lubrication. The role of nanoparticle concentration was also evident. Very low levels (<0.5 wt%) provide limited improvement, while excessive concentrations (>1.5–2 wt%) increase viscosity, clog nozzles, impair atomization, and can worsen surface finish and cutting forces. At moderate levels (up to 1 wt%), both nanofluids enhanced the thermal conductivity of the base fluid, leading to reductions in output parameters. Furthermore, the spherical morphology of nanoparticles, as reported by (Haghnazari and Abedini, 2021), contributed to improved lubrication by acting as micro-bearings between tool and chip, thereby reducing friction and stabilizing the machining process. A comparative summary is given in Table 16.

Table 16. Comparison table for both cases

Aspect	Case A: Al_2O_3 Nanofluid	Case B: ZnO Nanofluid
Dominant strength	Better cutting force and surface roughness reduction	Better cutting temperature reduction
Typical effect of wt%	Clear optimum; too high wt% increases viscosity and force/roughness	Similar optimum behaviour; strong effect on temperature
Sensitivity to cutting speed	Strong influence on temperature in both; Al_2O_3 gives lower forces at moderate speeds	High-speed performance enhanced by superior heat transfer
Best use-case	When priority is low force and high surface finish	When priority is aggressive cooling and thermal control

4. OPTIMIZATION AND VALIDATION

After statistical analysis of each input parameter on the output parameters was completed, the next work is to reach at optimum condition. (Mane *et al*. 2025) had suggested optimum condition using performed Taguchi Analysis. In this research, the optimal input and output parameter of level was identified using Box-Behnken method for RSM. Once the optimum level of parameters was recognized, the final task is to validate the predicted outputs with performing validation experiment. The aim of validating experiment is to verify conclusions derived in statistical analysis stage and improvement of measured output performance using optimum level.

The constraint criteria for the input parameters, namely cutting speed, wt% of NPs, and feed rate, were set within a defined range from lower to higher values. The output parameters, namely cutting force, cutting temperature, and surface roughness, were optimized with the objective of minimization. Table 17 shows constraint criteria for parameters to get optimum level.

Table 17. Criteria table for optimum condition

Parame-ter	Goal	Case A		Case B	
		Lower Limit	Upper Limit	Lower Limit	Upper Limit
A:CS	is in range	31.71	107.55	31.71	107.55
B:Wt% of NP	is in range	0	2	0	2
C:Fd	is in range	0.11	0.25	0.11	0.25
CF	minimize	129.16	407.78	101.31	408.66
CT	minimize	52.67	97.84	47	97.84
SR	minimize	2.252	5.211	2.194	4.563

For the Al_2O_3 nanofluid used as a cutting fluid, the optimum condition at a high desirability value of 0.941 for cutting force, cutting temperature, and surface roughness was obtained at a cutting speed of 31.71 m/min, 1 wt% of NPs, and a feed rate of 0.11. Similarly, for the ZnO nanofluid, the optimum condition at a desirability value of 0.815 for the same output parameters was achieved at a cutting speed of 31.71 m/min, 1.5 wt% of NPs, and a feed rate of 0.11. After determining the optimum conditions, confirmation experiments were conducted in three runs using the optimal levels of each input parameter.

Tables 18 and 19 show that the experimental results were compared with the predicted values. In Case A, the percentage errors between experimental and predicted values were 4.10% for cutting force, 7.62% for cutting temperature, and 11.55% for surface roughness. In Case B, the corresponding errors were 2.61%, 7.51%, and 8.14%, respectively. The predicted and measured values are in good agreement, indicating effective optimization of the control parameters.

Table 18. Combination of optimum parameters for confirmation experimentation run for case A

Output Parameter	Optimum Input Level	Predicted Value by RSM	Experiment Value
CF	CS: 31.71 m/min, wt% of NPs: 1 and Fd: 0.11 mm/rev	142.24	148.33
CT	CS: 31.71 m/min, wt% of NPs: 1 and Fd: 0.11 mm/rev	54.2	58.67
SR	CS: 31.71 m/min, wt% of NPs: 1 and Fd: 0.11 mm/rev	2.535	2.866

Table 19. Combination of optimum parameters for confirmation experimentation run for case B

Output Parameter	Optimum Input Level	Predicted Value by RSM	Experiment Value
CF	CS: 31.71 m/min, wt% of NPs: 1.5 and Fd: 0.11 mm/rev	148.45	152.43
CT	CS: 31.71 m/min, wt% of NPs: 1.5 and Fd: 0.11 mm/rev	37.09	40.1
SR	CS: 31.71 m/min, wt% of NPs: 1.5 and Fd: 0.11 mm/rev	3.046	3.316

5. CONCLUSION

The present investigation confirms that Al_2O_3 and ZnO mono nanofluids, applied through minimum quantity lubrication, improve the turning performance of AISI 1040 steel within the studied parameter range, with Case A (Al_2O_3 + MQL) identified as the most suitable cutting environment. The Box–Behnken design enabled the development of statistically adequate models for predicting cutting force, cutting temperature, and surface roughness. Case A showed greater reductions in cutting force and surface roughness due to the anti wear and friction reducing nature of Al_2O_3 nanofluid, while Case B (ZnO + MQL) provided better temperature control owing to its higher thermal conductivity. The choice between Case A and Case B depends on whether mechanical performance or thermal control is prioritized.

Mono nanofluid-based MQL is an effective and sustainable strategy for turning AISI 1040, with the RSM based Box–Behnken design enabling efficient multi response optimization. Al_2O_3 is preferred for better cutting force and surface finish, while ZnO offers superior temperature control, with optimal conditions at low speed, low feed, and around 1 wt% nanoparticles. However, the findings are limited to the studied parameter range, material, and setup, and do not consider tool wear, residual stress, long term stability, or cost and environmental analysis.

Abbreviations	
Al_2O_3	Aluminium Oxide
ANOVA	Analysis of Variance
ZnO	Zinc Oxide
NP	Nanoparticle
NF	Nanofluid
DOE	Design of Experimentation
RSM	Response surface methodology
wt%	Weight Fraction (%)
CS	Cutting Speed
Fd	Feed
CF	Cutting Force
CT	Cutting Temperature
SR	Surface Roughness

FUNDING

This research received no specific grant from any funding agency in the public, commercial, or not-for-profit sectors.

CONFLICTS OF INTEREST

The authors declare that there is no conflict of interest.

COPYRIGHT

This article is an open-access article distributed under the terms and conditions of the Creative Commons Attribution (CC BY) license (http://creativecommons.org/licenses/by/4.0/).

REFERENCES

Abhang, L. B. and Hameedullah, M., Experimental investigation of minimum quantity lubricants in alloy steel turning, *Int. J. Eng. Sci. Technol.,* 2(7), 3045–3053 (2010). https://shorturl.at/9mJrU

Agrawal, S. M. and Patil, N. G., Experimental study of non-edible vegetable oil as a cutting fluid in machining of M2 Steel using MQL, *Procedia Manufact.,* 20, 207–212 (2018). https://doi.org/10.1016/j.promfg.2018.02.030

Amrita, M., Shariq, S. A., Manoj, M. and Gopal, C., Experimental investigation on application of emulsifier oil-based nano cutting fluids in metal cutting process, *Procedia Eng.,* 97, 115–124 (2014). https://doi.org/10.1016/j.proeng.2014.12.231

Amrita, M., Srikant, R. R., Sitaramaraju, A. V., Prasad, M. M. S. and Krishna, P. V., Experimental investigations on influence of mist cooling using nanofluids on machining parameters in turning AISI 1040 steel, *Proc. Inst. Mech. Eng., Part J: J. Eng. Tribol.,* 227(12), 1334–1346 (2013). https://doi.org/10.1177/1350650113491934

Apmann, K., Fulmer, R., Soto, A. and Vafaei, S., Thermal Conductivity and Viscosity: Review and Optimization of Effects of Nanoparticles, *Mater*., 14(5), 1291 (2021). https://doi.org/10.3390/ma14051291

Bhadoria, N. S. and Bartarya, G., On the improvement in process performance of ceramic inserts during hard turning in MQL environment, *Mater. Manuf. Processes,* 37(3), 283-293 (2021). https://doi.org/10.1080/10426914.2021.1967978

Bumataria, R. K., Chavda, N. K. and Nalbandh, A. H., Performance evaluation of the cylindrical shaped heat pipe utilizing water-based CuO and ZnO hybrid nanofluids, *Energy Sour., Part A: Recovery, Util. Environ. Eff.,* 47(2), 1832628 (2020). https://doi.org/10.1080/15567036.2020.1832628

Bumataria, R. K., Chavda, N. K. and Panchal, H., Current research aspects in mono and hybrid nanofluid based heat pipe technologies, *Heliyon*, 5(5), e01627 (2019). https://doi.org/10.1016/j.heliyon.2019.e01627

Günan, F., Kıvak, T., Yıldırım, Ç. V. and Sarıkaya, M., Performance evaluation of MQL with Al_2O_3 mixed nanofluids prepared at different concentrations in milling of Hastelloy C276 alloy, *J. Mater. Res. Technol.,* 9(5), 10386–10400 (2020). https://doi.org/10.1016/j.jmrt.2020.07.018

Hadad, M. and Sadeghi, B., Minimum quantity lubrication-MQL turning of AISI 4140 steel alloy, *J. Cleaner Prod.,* 54, 332–343 (2013). https://doi.org/10.1016/j.jclepro.2013.05.011

Haghnazari, S. and Abedini, V., Effects of hybrid Al_2O_3–CuO nanofluids on surface roughness and machining forces during turning AISI 4340, *SN Appl. Sci*., 3(2) 203 (2021). https://doi.org/10.1007/s42452-020-04088-w

Haron, C. C. H., Ghani, J. A., Kasim, M. S., Soon, T. K., Gusri, A. I. and Sulaiman, M. A., Surface integrity of Inconel 718 under MQL condition, *Adv. Mater. Res*., 150–151, 1667–1672 (2011). https://doi.org/10.4028/www.scientific.net/AMR.150-151.1667

Hwang, Y. K. and Lee, C. M., Surface roughness and cutting force prediction in MQL and wet turning process of AISI 1045 using design of experiments, *J. Mech. Sci. Technol.,* 24(8), 1669–1677 (2010). https://doi.org/10.1007/s12206-010-0522-1

Khan, A. M., Jamil, M., Mia, M., Pimenov, D. Y., Gasiyarov, V. R., Gupta, M. K. and He, N., Multi-objective optimization for grinding of AISI D2 steel with Al_2O_3 wheel under MQL, *Mater.,* 11(11) 2269 (2018). https://doi.org/10.3390/ma11112269

Leppert, T., Effect of cooling and lubrication conditions on surface topography and turning process of C45 steel, *Int. J. Mach. Tools Manuf.,* 51(2), 120–126 (2011). https://doi.org/10.1016/j.ijmachtools.2010.11.001

Liu, Z. Q., Xu, J., Han, S. and Chen, M., A coupling method of response surfaces (CRSM) for cutting parameters optimization in machining titanium alloy under minimum quantity lubrication (MQL) condition, *Int. J. Precis. Eng. Manuf.,* 14(5), 693–702 (2013). https://doi.org/10.1007/s12541-013-0093-z

Montgomery, D. C., Design and analysis of experiments, 8th Ed. John Wiley and Sons, *Inc., New Jersey*, 486-497 (2013).

Mane, P. A., Dhawale, P. A., Nipanikar, S. and Khadtare, A. N., Predictive Modeling of Surface Roughness, Tool Wear, and Cutting Temperature in High-Speed Turning under Sustainable Machining Environments, *SAE Int. J. Mater. Manuf.,* 19(1), 95-115 (2025). https://doi.org/10.4271/05-19-01-0007

Padmini, R., Krishna, V. P., Mahith, S. and Kumar, S., Influence of Green Nanocutting Fluids on Machining Performance Using Minimum Quantity Lubrication Technique, *Mater. Today: Proc.,* 18, 1435-1449 (2019). https://doi.org/https://doi.org/10.1016/j.matpr.2019.06.612

Padmini, R., Vamsi, K. P. and Rao, G. K. M., Effectiveness of vegetable oil-based nanofluids as potential cutting fluids in turning AISI 1040 steel, *Tribol. Int.,* 94, 490–501 (2016). https://doi.org/10.1016/j.triboint.2015.10.006

Pasam, V. K., Srikant, R. R. and Gugulothu, S., Comparing the performance & viability of nano and microfluids in minimum quantity lubrication for machining AISI1040 steel, *Mater. Today: Proc.,* 5(2), 8016–8024 (2018). https://doi.org/10.1016/j.matpr.2017.11.486

Rao, S. N., Satyanarayana, B. and Venkatasubbaiah, K., Experimental estimation of tool wear and cutting temperatures in MQL using cutting fluids with CNT inclusion, *Int. J. Eng. Sci. Technol.,* 3(4), 2928–2931 (2011). https://shorturl.at/XCAyp

Rapeti, P., Pasam, V. K., Gurram, K. M. R. and Revuru, R. S., Performance evaluation of vegetable oil-based nano cutting fluids in machining using grey relational analysis-A step towards sustainable manufacturing, *J. Cleaner Prod.,* 172, 2862–2875 (2016). https://doi.org/10.1016/j.jclepro.2017.11.127

Saini, A., Dhiman, S., Sharma, R. and Setia, S., Experimental estimation and optimization of process parameters under minimum quantity lubrication and dry turning of AISI-4340 with different carbide inserts, *J. Mech. Sci. Technol.,* 28(6), 2307–2318 (2014). https://doi.org/10.1007/s12206-014-0521-8

Shaikh, M. B. N., Rosenkranz, A., Ali, M. and Ahmad, S. A., Improving the performance of cutting fluids by using ZnO and ZrO_2 nanoparticles, *Proc. Inst. Mech. Eng., Part N: J. Nanomater., Nanoeng. Nanosys.,* (2024). https://doi.org/10.1177/23977914241263453

Sharma, A. K., Singh, R. K., Dixit, A. R. and Tiwari, A. K., Characterization and experimental investigation of Al_2O_3 nanoparticle based cutting fluid in turning of AISI 1040 steel under minimum quantity lubrication (MQL), *Mater. Today: Proc.,* 3(6), 1899–1906 (2016a). https://doi.org/10.1016/j.matpr.2016.04.090

Sharma, A. K., Tiwari, A. K. and Dixit, A. R., Effects of Minimum Quantity Lubrication (MQL) in machining processes using conventional and nanofluid based cutting fluids: A comprehensive review, *J. Cleaner Prod.,* 127, 1–18 (2016b). https://doi.org/10.1016/j.jclepro.2016.03.146

Sharma, A. K., Tiwari, A. K., Singh, R. K. and Dixit, A. R., Tribological Investigation of TiO_2 Nanoparticle based Cutting Fluid in Machining under Minimum Quantity Lubrication (MQL), *Mater. Today: Proc.,* 3(6), 2155–2162 (2016c). https://doi.org/10.1016/j.matpr.2016.04.121

Sharma, V. S., Singh, G. and Sorby, K., A review on minimum quantity lubrication for machining processes, *Mater. Manuf. Processes,* 30(8), 935–953 (2015a). https://doi.org/10.1080/10426914.2014.994759

Sharma, V. S., Singh, G. and Sorby, K., A review on minimum quantity lubrication for machining processes, *Mater Manuf. Processes*, 30(8), 935–953 (2015b). https://doi.org/10.1080/10426914.2014.994759

Singh, G., Aggarwal, V. and Singh, S., Experimental investigations into machining performance of Hastelloy C-276 in different cooling environments, *Mater. Manuf. Processes*, 36(15), 1789–1799 (2021). https://doi.org/10.1080/10426914.2021.1945099

Sivaiah, P., Kumar, A. G. V., Narasimhamu, L. K. and Balaji, S. N., Performance improvement of turning operation during processing of AISI 304 with novel textured tools under minimum quantity lubrication using hybrid optimization technique, *Mater. Manuf. Processes,* 37(6), 693-700 (2021). https://doi.org/10.1080/10426914.2021.1967977

Sivaiah, P., Prasad, G. M., Singh M, M. and Uma, B., Machinability evaluation during machining of AISI 52100 steel with textured tools under Minimum Quantity Lubrication–A comparative study, *Mater. Manuf. Processes,* 35(15), 1761–1768 (2020). https://doi.org/10.1080/ 10426914.2020.1802034